



HAL
open science

Quantification of the Magnetic Anisotropy of a Single-Molecule Magnet from the Experimental Electron Density

Emil Damgaard-Møller, Lennard Krause, Kasper Tolborg, Giovanni Macetti, Alessandro Genoni, Jacob Overgaard

► **To cite this version:**

Emil Damgaard-Møller, Lennard Krause, Kasper Tolborg, Giovanni Macetti, Alessandro Genoni, et al.. Quantification of the Magnetic Anisotropy of a Single-Molecule Magnet from the Experimental Electron Density. *Angewandte Chemie International Edition*, 2020, 10.1002/anie.202007856 . hal-02913604

HAL Id: hal-02913604

<https://hal.univ-lorraine.fr/hal-02913604v1>

Submitted on 10 Aug 2020

HAL is a multi-disciplinary open access archive for the deposit and dissemination of scientific research documents, whether they are published or not. The documents may come from teaching and research institutions in France or abroad, or from public or private research centers.

L'archive ouverte pluridisciplinaire **HAL**, est destinée au dépôt et à la diffusion de documents scientifiques de niveau recherche, publiés ou non, émanant des établissements d'enseignement et de recherche français ou étrangers, des laboratoires publics ou privés.



A Journal of the Gesellschaft Deutscher Chemiker

Angewandte Chemie

GDCh

International Edition

www.angewandte.org

Accepted Article

Title: Quantification of the Magnetic Anisotropy of a Single-Molecule Magnet from the Experimental Electron Density

Authors: Emil Damgaard-Møller, Lennard Krause, Kasper Tolborg, Giovanni Macetti, Alessandro Genoni, and Jacob Overgaard

This manuscript has been accepted after peer review and appears as an Accepted Article online prior to editing, proofing, and formal publication of the final Version of Record (VoR). This work is currently citable by using the Digital Object Identifier (DOI) given below. The VoR will be published online in Early View as soon as possible and may be different to this Accepted Article as a result of editing. Readers should obtain the VoR from the journal website shown below when it is published to ensure accuracy of information. The authors are responsible for the content of this Accepted Article.

To be cited as: *Angew. Chem. Int. Ed.* 10.1002/anie.202007856

Link to VoR: <https://doi.org/10.1002/anie.202007856>

RESEARCH ARTICLE

Quantification of the Magnetic Anisotropy of a Single-Molecule Magnet from the Experimental Electron Density

Emil Damgaard-Møller,^[a] Lennard Krause,^[a] Kasper Tolborg,^[a] Giovanni Macetti,^[b] Alessandro Genoni,^[b] and Jacob Overgaard*^[a]

[a] E. Damgaard-Møller, Dr. L. Krause, K. Tolborg, Prof. Dr. J. Overgaard
Department of Chemistry
Aarhus University
Langelandsgade 140, 8000 Aarhus C.
E-mail: jacob@chem.au.dk

[b] Dr. G. Macetti, Dr. A. Genoni
Laboratoire de Physique et Chimie Théoriques (LPCT), UMR CNRS 7019
Université de Lorraine & CNRS
1 Boulevard Arago, F- 57078 Metz, France

Supporting information for this article is given via a link at the end of the document

Abstract: We report an entirely new application of the experimental electron density (EED) in the study of magnetic anisotropy of single-molecule magnets (SMMs). Among those SMMs based on one single transition metal, tetrahedral Co(II)-complexes are prominent, and their large zero-field splitting arises exclusively from coupling between the $d_{x^2-y^2}$ and d_{xy} orbitals. Using very low temperature single-crystal synchrotron X-ray diffraction data, we obtained an accurate electron density (ED) for a prototypical SMM, and we have used the experimental d-orbital populations to quantify the d_{xy} - $d_{x^2-y^2}$ coupling, which simultaneously provides us with the composition of the ground state Kramers doublet wave function. Based on this experimentally determined wave function, we calculate an energy barrier for magnetic relaxation in the range 193-268 cm^{-1} , which is in full accordance with the previously published value of 230 cm^{-1} obtained from near-infrared spectroscopy. These results provide the first clear and direct link between ED and molecular magnetic properties.

Introduction

Understanding of magnetic anisotropy remains a key factor in the development of well-performing single-molecule magnets (SMMs).^[1] Magnetic anisotropy arises from the interplay of ligand field and spin-orbit coupling (SOC) and acts to create an energy barrier for magnetic relaxation, which was first experimentally observed in a molecular cluster with twelve manganese ions (Mn_{12}).^[2] The theoretical foundation for magnetic anisotropy is firmly established for transition metal SMMs,^[3] and depends on whether orbital angular momentum is quenched or not.

Orbital angular momentum in transition metal compounds is associated with the $(d_{xy}, d_{x^2-y^2})$ and (d_{yz}, d_{xz}) orbital pairs as they are linear combinations of the $m_l = (\pm 2)$ and (± 1) functions, respectively.^[4] Thus, an odd number of electrons in the degenerate pairs $(d_{xy}, d_{x^2-y^2})$ or (d_{yz}, d_{xz}) would contribute with angular momentum $L=2$ or $L=1$, respectively, due to their multi-configurational nature, whereas $(d_{xy}, d_{x^2-y^2})^2$ or $(d_{yz}, d_{xz})^2$ electronic configurations lead to $L=0$ due to the Pauli exclusion principle. In

other words, quenching of the orbital momentum is associated with the lifting of the degeneracy of these two orbital pairs.

An unquenched orbital angular momentum will yield a large spontaneous splitting of the magnetic states in zero magnetic field, called zero-field splitting (ZFS). The size of this splitting quantifies the magnetic anisotropy of the system, and thus governs the height of the energy barrier for magnetic relaxation. In these cases, the ZFS is determined from the coupled spin and orbital angular momentum, generating M_J states, and it can be calculated *a priori*.^[4] For any given molecule, partial quenching of the orbital angular momentum will lead to a decrease in the ZFS, explaining why significant effort is given to the design of molecules, in which the entire orbital angular momentum is preserved. This is, however, a tricky task, since the d-orbitals are strongly influenced by the ligand field because of their diffuse nature.^[5] Therefore, this was achieved only for a few molecular geometries, for example, linear SMMs.^[6] Recently, a linear dialkyl Co(II) complex was reported showing a maximal orbital angular momentum of $L=3$ due to a $(d_{xy}, d_{x^2-y^2})^3 (d_{yz}, d_{xz})^3 (d_{zz})^1$ ground state configuration,^[7] hereby achieving the largest theoretically possible ZFS for a Co(II) ion.

When the orbital angular momentum is quenched by the ligand field, it can be reintroduced through the spin-orbit coupling (second-order orbital angular momentum). In such cases, L is no longer a good quantum number, and the system is treated as a pure spin system with spin-Hamiltonians (eq. 1), with the ZFS parameters (D and E) describing any splitting of the M_s states arising from effects of the SOC.^[8]

$$\hat{H}_{ZFS} = \vec{S} \cdot \bar{D}' \cdot \vec{S}, \quad (1)$$

where \bar{D}' is a 3x3 tensor, which, when diagonalized and made traceless, gives the ZFS parameters as $D = 3/2 \cdot D'_{zz}$ and $E = 1/2(D'_{xx} - D'_{yy})$. The \bar{D}' -tensor can be approximated from second order perturbation theory as,

$$D'_{ab} = -\lambda^2 \sum_{K \neq 0} \frac{\langle 0 | \hat{L}_a | K \rangle \langle K | \hat{L}_b | 0 \rangle}{E_K - E_0} \quad (2)$$

RESEARCH ARTICLE

where λ is the atomic SOC constant, $|0\rangle$ is the spin-orbit free ground state, $|K\rangle$ represents the K-th excited state, and $\hat{L}_{a,b}$ ($a, b = x, y, z$) is the orbital angular momentum operator. From eq. 1 and eq. 2 it is possible to establish a relationship between the ligand field splitting (i.e., d-orbital splitting) and the ZFS, which allows for design strategies for obtaining well-performing SMMs. These strategies rely on the minimization of the energy difference (denominator in eq. 2) between orbitals coupled through the \hat{L}_z operator, or in other words minimizing the quenching of orbital angular momentum. For a more elaborate explanation, we refer the reader to other relevant literature on this topic.^[3, 9]

The ligand field splitting is often estimated from theoretical calculations, as d-orbitals and their energies are not physical observables. However, using high-resolution single-crystal X-ray diffraction data to model an atom-centered experimental electron density (EED) following the Hansen-Coppens multipole formalism^[10] provides rich information about a wide range of molecular and solid-state properties.^[11] For instance, it is possible to project the EED in close proximity of the metal center onto atomic d-orbital functions,^[12] thus leading to experimental d-orbital populations. This procedure represents the only known experimental technique to quantify the d-orbital populations, but up to now, only a few EED studies of SMMs have been reported.^[13] Nevertheless, given information on the d-orbital populations, and thereby indirectly the ligand field splitting, an estimation of the ZFS should be within reach.

In this contribution, we investigate the compound $(\text{HNEt}_3)_2[\text{Co}^{\text{II}}(\text{L}^2)_2]$ (**1**), where $\text{H}_2\text{L} = \text{bis}(\text{methanesulfonamido})\text{-benzene}$ first published by Rechkemmer *et al.*^[14] Compound **1** shows extraordinary SMM properties with a quenched orbital angular momentum, but an unusually large ZFS. The authors ascribed this to a significant stabilization of the d_{xy} -orbital, due to a highly distorted local coordination geometry around cobalt. This stabilization increases the contribution to D_{zz} (and hence D) as the \hat{L}_z operator couples the d_{xy} and $d_{x^2-y^2}$ orbitals and the energy separation between these orbitals becomes very small in **1** (see Figure 1b).

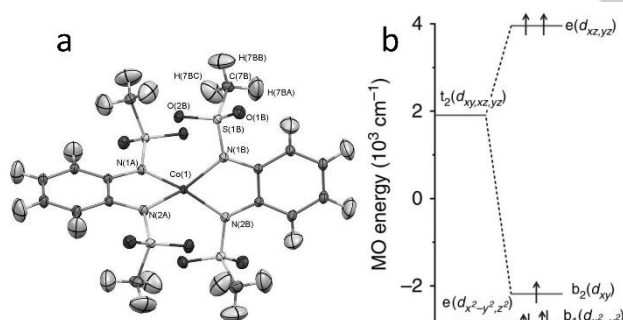


Figure 1. a) Molecular anion of **1** shown with 90% probability ellipsoids. Labels of representative atoms indicate color scheme. Counter-ion not shown. b) d-orbital energy diagram for **1** in D_{2d} symmetry, adapted from ref. ^[14].

In the present work, we propose a fundamentally new way of determining the energy barrier to magnetic relaxation, using the d-orbital populations obtained from a multipole model (MM) refined against single-crystal X-ray diffraction data. The work-flow is schematized in Figure 2, where the important part of the work is to establish the correlation between the d-orbital populations and the SOC wave function, and establish a prediction of the ZFS

from the SOC wave function of the ground state. In Figure 2, each step has been assigned a letter (a-g) for easy reference.

In the paper, we first briefly comment on the structure of the compound. Then we describe the *ab initio* calculation, and the SOC wave function obtained from it, and furthermore describe the correlation between the obtained calculation results and the d-orbital populations ($e \rightarrow f \rightarrow c$). From a large set of *ab initio* calculations of different tetrahedral Co(II) compounds, we are then able to establish a correlation between the ground state SOC wave function and the ZFS ($f \rightarrow g$).

In order to verify that the projection of the Hansen-Coppens multipole formalism to the d-orbital functions provides accurate d-orbital populations, we generate theoretical structure factors from the SOC wave function, and obtain the d-orbital populations from the theoretical electron density ($f \rightarrow d \rightarrow c$). Doing so, we can directly compare the predicted d-orbital populations from the SOC wave function ($e \rightarrow f \rightarrow c$) and the Hansen-Coppens multipole formalism ($e \rightarrow f \rightarrow d \rightarrow c$), to show their consistency. With this established, we turn our focus to the experimental ED, where our main focus is the d-orbital populations (the experimental description and modelling ($a \rightarrow b \rightarrow c$) is described in detail in the SI). A direct conversion from the d-orbital populations to the ZFS ($c \rightarrow f \rightarrow g$) is not unique, since approximations are necessary in order to obtain the SOC wave function from the d-orbital populations ($c \rightarrow f$).

Results and Discussion

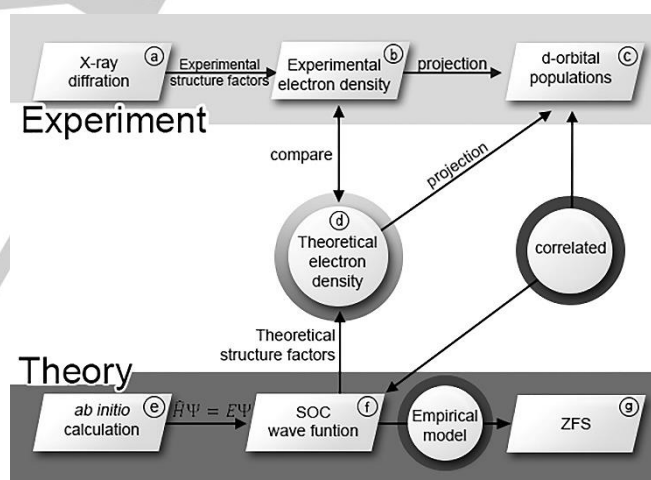


Figure 2. Illustration of the work-flow in the current work, showing the possible path from single crystal diffraction data to ZFS.

The solid-state structure of **1** was determined by synchrotron radiation single-crystal X-ray diffraction measured at 20 K, and the structure of the complex anion is shown in Figure 1a (exact experimental procedure is described in SI). The geometry of the first coordination sphere of Co(II) can be described as a distorted tetrahedron where the distance between two pairs of nitrogen atoms is reduced to give D_{2d} symmetry mediated by the rigid geometry of the bidentate ligand. Such geometrical distortion has previously been shown to give significantly enhanced SMM properties.^[15] Furthermore, the two bidentate ligands are rotated such that the angle between the planes spanned by N(1A)-Co-N(2A) and N(1B)-Co-N(2B) (screw-angle) slightly deviates from 90° required for strict D_{2d} symmetry, and thereby the molecule

RESEARCH ARTICLE

exhibits no true symmetry (C_1). Selected structural details can be found in Table 1, and the overall structural details are consistent with the previous structural report.^[14]

Table 1. Crystallographic information and selected bond distance and angles for **1**

Crystallographic information		Bond distances (Å) and angles (°)	
Formula	$C_{28}H_{52}CoN_6O_8S_4$	Co-N(1A)	2.0230(3)
Weight, g mol ⁻¹	787.94	Co-N(2A)	2.0142(2)
Crystal system	Orthorhombic	Co-N(1B)	2.0216(3)
Space group	$P2_12_12_1$	Co-N(2B)	2.0096(3)
Z	4		
a, Å	12.161 (2)	N(1A)-Co-N(2A)	80.543(11)
b, Å	15.995 (2)	N(1B)-Co-N(2B)	80.657(10)
c, Å	18.301 (3)	N(1A)-Co-N(1B)	121.337(7)
T, K	20	N(1A)-Co-N(2B)	127.949(11)
ρ , g cm ⁻³	1.470	N(2A)-Co-N(1B)	128.213(9)
μ mm ⁻¹	0.06	N(2A)-Co-N(2B)	124.858(9)
d_{\min} , sin θ/λ	0.35, 1.43		
N_{meas}	1226445	Screw-angle	85.10(1)
N_{uniq}	86421		
R_{int} , R_{pim}	0.0486, 0.0114		
N_{obs} , N_{var}	80330, 651		
$R(F)$, $R_w(F^2)$	0.0124, 0.0167		
goodness-of-fit	1.0417		
$\Delta\rho_{\text{max}}$, $\Delta\rho_{\text{min}}$ (e Å ⁻³)	0.492, -0.316		

CASSCF(7,5) and NEVPT2 calculations were performed with the DKH-def2-TZVP basis-set using the ORCA software^[16] on the molecular anion of **1** using the geometry obtained from the X-ray diffraction experiment (see SI for more details about the calculations). These computations provide information about the electronic nature of the ground state and the SOC, and are the best estimates of the true electronic structure. In the following, we report the results ($e \rightarrow f \rightarrow c$ in Figure 2).

The energies and states obtained from the calculations, including the d-orbital splitting scheme that is shown in Figure 1b, closely resemble those that were previously reported for this compound.^[14] In Figure 3, the calculation results are summarized, and we observe the well-known splitting of the 4F ground state of a free d^7 -ion upon application of a tetrahedral crystal field into $^4A_{2g}$, $^4T_{2g}$, and $^4T_{1g}$ states. When the symmetry is lowered to D_{2d} by the distortion described above, the $^4T_{2g}$ term splits significantly, such that the 4B_2 state shifts closer to the ground state (4B_1). In the D_{2d} point group, these two states, which are by symmetry only allowed to couple through the \hat{L}_z operator,^{[17][18]} are associated with the following electron configurations (and hence d-orbital populations):

$$^4B_1 : d_{xy}^1 d_{yz}^1 d_{z^2}^2 d_{xz}^1 d_{x^2-y^2}^2$$

$$^4B_2 : d_{xy}^2 d_{yz}^1 d_{z^2}^2 d_{xz}^1 d_{x^2-y^2}^2$$

When the *ab initio* ligand field theory (AILFT)^[19] program in ORCA is used, the CASSCF active space is rotated such that the natural orbitals are in accordance with the input coordinate system to yield atomic d-orbitals. The intuitive understanding of the resulting CASSCF wave functions thus depends on the input coordinate system, which should be chosen in a chemically meaningful way. In our case, the coordinate system corresponds to the principal axes of the D_{2d} point group (z-axis from cobalt to in-between N(1A)-N(2A), and x- and y-axis in-between N(2A)-N(1B) and N(1A)-N(1B), respectively). This allows for a straightforward analysis of the Slater determinants in the CASSCF expansions, as the occupancies are referring to the atomic d-orbitals.

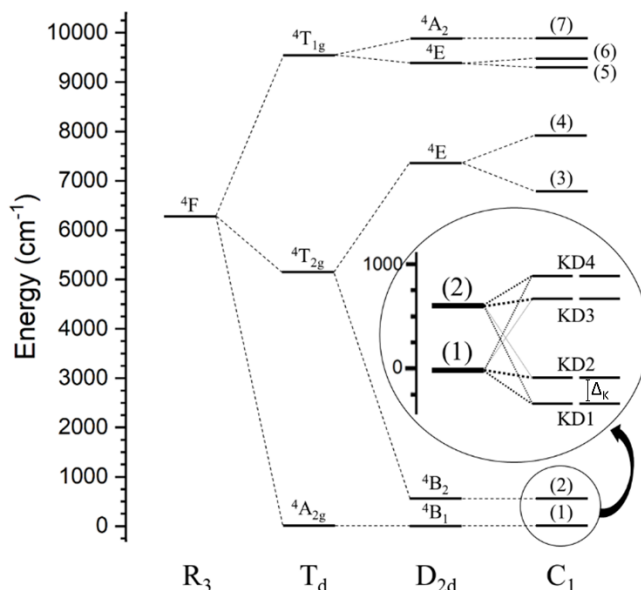


Figure 3. Energy level diagram of the 4F ground term, constructed from the results of the CASSCF(7,5), NEVPT2 calculation using the DKH-def2-TZVP basis-set based on the true symmetry (C_1) and then constructed from the appropriate barycenters of the states. R_3 is the spherical point group associated with the free ion, T_d is the cubic point group associated with a perfect tetrahedral crystal field, the D_{2d} point group is achieved by compressing the ligands pairwise as described in the text, and C_1 is the actual point group symmetry of the complex anion. The energies are shifted in such a way that the ground state (1) energy corresponds to 0 cm^{-1} . The detailed SOC-splitting of states (1) and (2) into four Kramers' doublets are shown in the enlarged circular inset.

The resulting CASSCF wave functions clearly show that the symmetry lowering from D_{2d} to C_1 (see Figure 3) did not significantly alter the composition of the two lowest CASSCF states, as the states consist almost exclusively of single Slater determinants (the full table is available in Table S2 in the SI):

$$(1) : 99.8\% d_{xy}^1 d_{yz}^1 d_{z^2}^2 d_{xz}^2 d_{x^2-y^2}^2 ; (2) : 99.7\% d_{xy}^2 d_{yz}^1 d_{z^2}^2 d_{xz}^2 d_{x^2-y^2}^2$$

Therefore, states (1) and (2) can be associated with 4B_1 and 4B_2 . After the application of SOC in the *ab initio* calculation, the resulting Kramers' doublets (KDs) are linear combinations (given below as $w \cdot |(state), M_S\rangle$) of the states (1) and (2), whereas no higher-lying states are mixed into the Kramers' doublets due to the large energy separation to 4E . The two lowest KDs, seen in the enlarged circular inset in Figure 3, originating from (1) are:

$$KD1 : 0.737 \cdot |^4B_1, \pm 3/2\rangle + 0.261 \cdot |^4B_2, \pm 3/2\rangle$$

$$KD2 : 0.916 \cdot |^4B_1, \pm 1/2\rangle + 0.073 \cdot |^4B_2, \pm 1/2\rangle$$

We have quantified the composition of the KDs using the weights of the states and not the coefficients (for these, see Table S3 in SI), as the former represents the probability of a given state, and therefore are directly linked to the ED. The average electron configurations of the two KDs (i.e., the d-orbital populations) are then obtained as the sum of the product of the weights and the electron configurations of the corresponding states (an example is provided in Note S1 in the SI). This leads to the following expressions for the d-orbital populations of the KDs:

RESEARCH ARTICLE

$$\begin{aligned}
 KD1 &: d_{xy}^{1.261} d_{yz}^1 d_{z^2}^2 d_{xz}^1 d_{x^2-y^2}^{1.737} \\
 KD2 &: d_{xy}^{1.073} d_{yz}^1 d_{z^2}^2 d_{xz}^1 d_{x^2-y^2}^{1.916},
 \end{aligned}$$

Now we turn our attention to the prediction of the ZFS from the SOC wave function ($f \rightarrow g$). Since the diffraction experiment is performed at very low temperatures (20 K), only KD1 will be populated. Thus, in order to extract the energy barrier from the EED (i.e., the magnetically important energy difference between KD1 and KD2, from now on referred to as Δ_K , which is linked to the barrier to magnetic relaxation via the Orbach process), we need to establish a relationship between the d-orbital populations of KD1 and Δ_K .

To achieve this, let us consider two extremes. First, if 4B_1 and 4B_2 are infinitely far apart, equivalent to a very large energy separation between $d_{x^2-y^2}$ and d_{xy} , no coupling occurs, Δ_K is zero (given that no other coupling is present), and KD1 and KD2 would exhibit identical d-orbital populations $d_{xy}^1 d_{yz}^1 d_{z^2}^2 d_{xz}^1 d_{x^2-y^2}^2$ corresponding to the 4B_1 state. At the other extreme, we find the case where 4B_1 and 4B_2 are degenerate, or equivalently that $d_{x^2-y^2}$ and d_{xy} are degenerate. In this scenario, the d-orbital populations for both KD1 and KD2 would be $d_{xy}^{1.5} d_{yz}^1 d_{z^2}^2 d_{xz}^1 d_{x^2-y^2}^{1.5}$ and hence the ground state would thus have $L = 2$, leading to $\Delta_K = 343 \text{ cm}^{-1}$ from first-order SOC.^[20] In-between these extremes we hypothesize the presence of a correlation between the degree of coupling, reflected in the d-orbital populations, and the size of Δ_K .

To examine this correlation we performed *ab initio* CASSCF(7,5) calculations on a large series of cobalt(II) based molecules with approximate D_{2d} symmetry, all of which shared the same features of **1**, i.e., that the spin-orbit free states (1) and (2) could be associated with 4B_1 and 4B_2 . Upon plotting the calculated Δ_K against the coefficient of 4B_2 (i.e., $\sqrt{w({}^4B_2)}$) in KD1, we observed a linear relationship that could be convincingly fitted using the following expression with $R^2 = 0.9958$ (see the SI):

$$\Delta_K = 588 \sqrt{w({}^4B_2)} \text{ cm}^{-1} - 76 \text{ cm}^{-1} \quad (3)$$

It is clear that this relationship is only valid when the coupling of states (1) and (2) is significant, as eq. 3 does not predict $\Delta_K = 0$ for $w({}^4B_2) = 0$. Nevertheless, given this relationship we are able to quantify the barrier for magnetic relaxation directly from the experimental d-orbital populations, as they provide information of $w({}^4B_2)$ in distorted tetrahedral Co(II) complexes.

To date, d-orbital populations obtained from a MM of X-ray diffraction experiments have been used qualitatively to address trends, but to our knowledge, never quantitatively. Therefore, we need to ensure that the Hansen-Coppens multipole formalism is actually capable of producing accurate d-orbital populations. To verify this, we use theoretical structure factors (TSFs). Recent progress in computational methods has provided access to precise ED from spin-orbit coupled states from an *ab initio* calculation,^[16] and we subsequently obtain TSFs from a Fourier transformation of the ED.^[21] Using these TSFs, we obtain a theoretical ED-model (TED) using the MM formalism, and examine whether this MM gives d-orbital populations comparable to those predicted directly from the wave function composition of the KDs, seen in column 2 and 3 in Table 2 ($f \rightarrow d \rightarrow c$ in Figure 2).

The TSFs were calculated from the Boltzmann-averaged ED of KD1 and KD2 at 20 K (which is nearly identical to the ED of KD1, as the Boltzmann ratio is $9.8 \cdot 10^6$ at 20 K). TSFs from the ED of KD2 were also produced, reflecting the ED of the first excited state. The resulting d-orbital populations are given in Table 2, while details of the MM refinements are given in the SI. There is a striking agreement between the MM d-orbital populations (columns 4 & 5) and the predicted electron configurations for KD1 and KD2 (columns 2 & 3) for d_{z^2} , $d_{x^2-y^2}$, and d_{xy} . The small deviation from 1.0 electron in d_{yz} and d_{xz} in columns 4 & 5 can be ascribed to the fact that these form anti-bonding orbitals in this compound, and thus receive some electrons from the ligands involved in the relevant covalent interactions. We note that the slight increase in these two orbitals matches precisely the increase in the total population of the d-shell.

Thus, we conclude that the MM can provide d-orbital populations with extraordinary accuracy. However, it includes the effects of metal-ligand charge transfer that are not accounted for in the simple prediction from the *ab initio* wave function.

Table 2. d-orbital populations obtained from the direct analysis of the *ab initio* results of KD1 and KD2 (columns 2 & 3), from the multipole refinement using theoretical structure factors produced from KD1 and KD2 (columns 4 & 5) and experimental structure factors (column 6). Important values are highlighted in bold font for the “*Ab initio* prediction” and “Theoretical structure factors”, and the difference in d-orbital populations between experiment and KD1 obtained from TSFs is shown in the last column. Accumulation of errors based on the refined multipole parameters have provided the uncertainties given in parentheses in column 6.

	Ab initio prediction		MM - TED		MM - EED	
	KD1	KD2	KD1	KD2	d-pop	EED-TED(KD1)
d_{yz}	1.000	1.000	1.060	1.063	1.200(7)	0.140
d_{xz}	1.000	1.000	1.092	1.095	1.209(7)	0.117
d_{xy}	1.261	1.073	1.266	1.083	1.423(7)	0.157
$d_{x^2-y^2}$	1.737	1.916	1.739	1.921	1.790(7)	0.051
d_{z^2}	2.000	2.000	1.993	1.989	1.867(7)	-0.126
Total	6.998	6.989	7.151	7.152	7.489	0.337

It should be noted that it is of great importance to use the same radial functions in the MM that is used in the *ab initio* calculation. Otherwise, the assumption that the transformation between multipole population parameters and d-orbital populations builds on becomes invalid.^[12] We note this here, as this is not the default in the used MM software, where single-zeta Slater functions are commonly used rather than the ones derived from atomic wave functions (see SI for further details).

We now turn our attention to the experimentally obtained d-orbital populations, which, if they were correct and the experiment is flawless, should give populations identical to those for the electronic ground state, KD1. As we have shown recently, the use of novel detector technologies in combination with synchrotron X-ray sources allows us to obtain extremely accurate data and, subsequently, highly reliable EED models,^[22] and we are therefore confident that the data quality is state-of-the-art. However, numerous published EED studies have presented reliable d-orbital populations based on less accurate data.

The experimental populations are listed in Table 2, column 6, along with the deviation from KD1-populations in column 7. The

RESEARCH ARTICLE

experimental results for **1** correctly predict the relative d-orbital energies as $d_{z^2} < d_{x^2-y^2} < d_{xy} < d_{xz} \approx d_{yz}$, from the assumption that a larger population corresponds to a stabilization of a given orbital, in complete accordance with Figure 1b. Furthermore, the large population of the d_{xy} orbital is an indication of the significant coupling of the $d_{x^2-y^2}$ and d_{xy} orbitals, i.e., close proximity of states (1) and (2).

Instead of jumping directly to an experimental estimate of Δ_K from the raw d-orbital populations, we need to consider whether the observed differences in d-orbital populations between TED(KD1) and experiment necessitates a modification of the populations (Figure 4).

Firstly, the total population of all d-orbitals is 0.337e larger for the experimental d-orbital populations compared to the TED, indicating an increased electron donation from the ligands to the metal center. There are no indications that this results from the use of the MM as the *ab initio* populations are the same as the ones from TED, and it is, therefore, reasonable to assume that all the extra electrons found in the EED result from donation to the anti-bonding d_{yz} and d_{xz} orbitals. However, after subtracting the excess electrons in the d_{yz} and d_{xz} orbitals from the total ($7.489 - 0.209 - 0.200 = 7.08$), we still have an excess of 0.08 electrons. The only reasonable origin for this must be charge transfer to d_{xy} , indicating that this orbital is partly anti-bonding, contrary to the *ab initio* results, whereas d_{z^2} and $d_{x^2-y^2}$ are non-bonding. Therefore, we subtract 0.08e from the d_{xy} population, and are left with modified d-orbital populations, in which all electron transfer effects have been removed, and thus should reflect the best estimate of populations directly comparable with the *ab initio* prediction:

$$d_{xy}^{1.343} d_{yz}^1 d_{z^2}^{1.867} d_{xz}^1 d_{x^2-y^2}^{1.790}$$

This modification process is sketched in Figure 4.

Secondly, we note that although the d_{z^2} and $d_{x^2-y^2}$ orbitals are not allowed to couple through any of the $\hat{L}_{x,y,z}$ operators, the experimental d_{z^2} population differs significantly from the expected value of 2.0. There are two possible explanations for this: 1) electron density has been transferred from d_{z^2} to $d_{x^2-y^2}$ due to the near-degeneracy of the two orbitals (Figure 1b), even though this is theoretically forbidden. This assumption suggests that 0.126e have been transferred to $d_{x^2-y^2}$; or 2) it could be due to the symmetry-allowed mixing of $3d_{z^2}$ and $4s$ orbitals, which has previously been shown to decrease the d_{z^2} orbital population and does not add any electrons to the other d-orbitals.^[13b] These two cases are considered below in cases C and B, respectively.

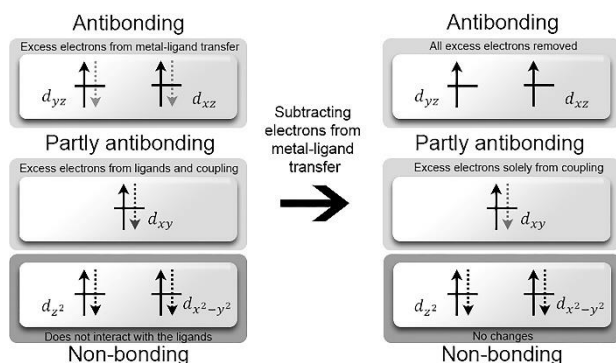


Figure 4. Schematized modification of the d-orbital populations. The dashed arrows symbolize the fractional electrons in the d-orbital populations (i.e., the population exceeding 1.0e). Here some electrons in the d_{xy} orbital are removed

in the subtraction, indicated by a slightly more transparent dashed arrow in the right scheme.

We find three equally good estimates (A-C) for the ground state wave functions, and thus the ZFS, all starting from the modified populations (path c→f in Figure 2):

A. We make no further alterations to the populations and assume that the population of 1.79 in the $d_{x^2-y^2}$ represents the weight (0.79) of the ground state 4B_1 , and that the remaining contribution is from the first excited state 4B_2 . In doing so, we obtain the following wave function for the ground state (GS):

$$GS(A) : 0.790 \cdot |{}^4B_1\rangle + 0.210 \cdot |{}^4B_2\rangle$$

B. We assume the missing electrons in d_{z^2} are due to the $3d - 4s$ mixing and, therefore, it does not affect the d_{xy} and $d_{x^2-y^2}$ orbitals. By taking the populations of the d_{xy} and $d_{x^2-y^2}$ orbitals, we get the wave function $0.790 \cdot |{}^4B_1\rangle + 0.343 \cdot |{}^4B_2\rangle$, which after normalization gives:

$$GS(B) : 0.724 \cdot |{}^4B_1\rangle + 0.276 \cdot |{}^4B_2\rangle$$

C. The missing electrons in d_{z^2} are due to interaction with $d_{x^2-y^2}$ and are thus subtracted from the $d_{x^2-y^2}$ population, giving the electron configuration $d_{xy}^{1.343} d_{yz}^1 d_{z^2}^1 d_{xz}^1 d_{x^2-y^2}^{1.657}$, which leads to the following wave function:

$$GS(C) : 0.657 \cdot |{}^4B_1\rangle + 0.343 \cdot |{}^4B_2\rangle$$

By applying the empirically observed relationship between ground state electron configuration and Δ_K (eq. 3) we find the barriers 193, 233, and 268 cm^{-1} for the three situations A-C.

This is a fascinating result as it outlines the composition of the lowest Kramers doublet as well as the energy splitting between the two lowest Kramers doublets. Intriguingly, this is based exclusively on the EED model combined with the well-established fact that only $d_{x^2-y^2}$ and d_{xy} orbitals are involved in the splitting of the lowest Kramers doublets in these distorted tetrahedral Co(II) complexes.^[14-15, 23] Furthermore, the predicted energy-splitting interval, 193-268 cm^{-1} , contains very well the value of 230 cm^{-1} previously obtained from *ab initio* calculations, NIR-spectroscopy, and DC magnetometry.^[14]

The analysis protocol presented herein shows the unexploited potential of modern ED-related experiments. In this work, the energy barrier is analyzed solely from the perspective of the 'degree of coupling' between two orbitals. We find this intriguing, as this model is valid for molecules both with an unquenched and with a quenched orbital angular momentum. The ZFS parameters D and E that are usually reported for these types of complexes^[24] can include any effects arising from the spin-orbit coupling, thus lacking interpretability, whereas the coupling in this work is directly evaluated.

Lastly, we note that a topological analysis of the EED locates bcps between oxygen atoms and the hydrogen atoms on the methyl groups directly bonded to sulfur. This O...H bond is a weak, but well-known interaction,^[25] and is an excellent explanation for the driving force behind the deviation away from D_{2d} symmetry. Exchanging the hydrogen atoms of the methyl groups with more electronegative atoms such as fluorine would possibly hinder the appearance of this intramolecular interaction, and potentially lead to a more symmetrical molecule.

Conclusion

RESEARCH ARTICLE

With the new improvements in detector technologies, combined with low temperatures and synchrotron radiation, we have obtained extremely high-quality diffraction data that enabled the modeling of the EED distribution in **1**, leading to experimental d-orbital populations. Theoretical structure factors generated from a calculated wave function showed that the Hansen-Coppens multipole formalism is capable of reproducing the expected d-orbital populations from an *ab initio* calculation to an unprecedented accuracy, paving the way for a more rigorous and quantitative analysis of the d-orbital populations.

The experimental and theoretical d-orbital populations differed significantly from each other, and an analysis of the differences showed that the metal-ligand charge transfer was more substantial than what was estimated from the TED. More importantly, we obtained a direct relationship between Δ_K and the ground state SOC wave function composition, making it possible to determine Δ_K directly from the d-orbital populations of an EED. By analyzing the barrier for magnetic relaxation this way, we enable an equal treatment for SMMs exhibiting both quenched and unquenched orbital momenta. Here we note that this analysis is valid only for compounds where the coupling of the d_{xy} and $d_{x^2-y^2}$ orbitals is solely responsible for the ZFS, but we believe that it can be extended to include all possible couplings. Research on that front is currently the focus of our lab.

We will continue to explore the potential of diffraction methods in molecular magnetism, and we believe that the current study will serve as an excellent example of the kind of information that can be obtained from ED experiments.

Acknowledgements

This work was supported by grants from VILLUM FONDEN (12391) and the Danish National Research Foundation (DNRF-93). Affiliation with the Center for Integrated Materials Research (iMAT) at Aarhus University is gratefully acknowledged. The synchrotron experiment was performed on beamline BL02B1 at SPring-8 with the approval of the Japan Synchrotron Radiation Research Institute as a Partner User (proposal no. 2018B0078).

Keywords: d-orbital populations • electron density • magnetic properties • single-molecule magnets • X-ray diffraction

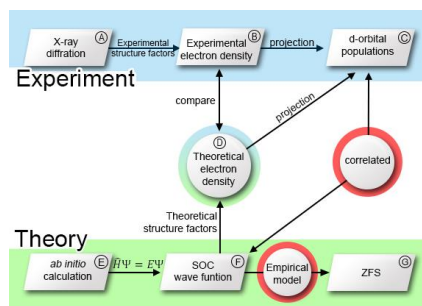
Abbreviations

AiLFT - *ab initio* ligand field theory
 CASSCF - Complete active space self-consistent field
 ED - Electron density
 EED - Experimental electron density
 GS - Ground state
 KD - Kramers doublet
 MM - Multipole model
 NEVPT2 - N-electron valence state perturbation theory
 SMM - Single-molecule magnet
 SOC - Spin-orbit coupling
 TED - Theoretical electron density
 TSF - Theoretical structure factor
 ZFS - Zero-field splitting

- [1] a) O. Waldmann, *Inorg. Chem.* **2007**, *46*, 10035-10037; b) E. Ruiz, J. Cirera, J. Cano, S. Alvarez, C. Loose, J. Kortus, *Chem. Commun.* **2008**, 52-54.
- [2] R. Sessoli, D. Gatteschi, A. Caneschi, M. A. Novak, *Nature* **1993**, *365*, 141-143.
- [3] S. Gomez-Coca, E. Cremades, N. Aliaga-Alcalde, E. Ruiz, *J. Am. Chem. Soc.* **2013**, *135*, 7010-7018.
- [4] B. N. Figgis, M. A. Hitchman, *Ligand field theory and its applications*, Wiley-VCH, New York, **2000**.
- [5] P. P. Power, *Chem. Rev.* **2012**, *112*, 3482-3507.
- [6] a) J. M. Zadrozny, M. Atanasov, A. M. Bryan, C.-Y. Lin, B. D. Rekker, P. P. Power, F. Neese, J. R. Long, *Chem. Sci.* **2013**, *4*, 125-138; b) J. M. Zadrozny, D. J. Xiao, M. Atanasov, G. J. Long, F. Grandjean, F. Neese, J. R. Long, *Nat. Chem.* **2013**, *5*, 577-581; c) X. N. Yao, J. Z. Du, Y. Q. Zhang, X. B. Leng, M. W. Yang, S. D. Jiang, Z. X. Wang, Z. W. Ouyang, L. Deng, B. W. Wang, S. Gao, *J. Am. Chem. Soc.* **2017**, *139*, 373-380.
- [7] P. C. Bunting, M. Atanasov, E. Damgaard-Møller, M. Perfetti, I. Crassee, M. Orlita, J. Overgaard, J. van Slageren, F. Neese, J. R. Long, *Science* **2018**, *362*, eaat7319.
- [8] R. Boca, *Coord. Chem. Rev.* **2004**, *248*, 757-815.
- [9] R. Ruamps, L. J. Batchelor, R. Maurice, N. Gogoi, P. Jimenez-Lozano, N. Guihery, C. de Graaf, A. L. Barra, J. P. Sutter, T. Mallah, *Chem. Eur. J.* **2013**, *19*, 950-956.
- [10] N. K. Hansen, P. Coppens, *Acta Cryst. A.* **1978**, *34*, 909-921.
- [11] a) D. Stalke, *Chem. Eur. J.* **2011**, *17*, 9264-9278; b) M. S. Schmokel, J. Overgaard, B. B. Iversen, *Z. Anorg. Allg. Chem.* **2013**, *639*, 1922-1932; c) K. Tolborg, B. B. Iversen, *Chem. Eur. J.* **2019**, *25*, 15010-15029.
- [12] A. Holladay, P. Leung, P. Coppens, *Acta Cryst.* **1983**, *A39*, 377.
- [13] a) M. Craven, M. H. Nygaard, J. M. Zadrozny, J. R. Long, J. Overgaard, *Inorg. Chem.* **2018**, *57*, 6913-6920; b) M. K. Thomsen, A. Nyvang, J. P. S. Walsh, P. C. Bunting, J. R. Long, F. Neese, M. Atanasov, A. Genoni, J. Overgaard, *Inorg. Chem.* **2019**, *58*, 3211-3218; c) C. Gao, A. Genoni, S. Gao, S. Jiang, A. Soncini, J. Overgaard, *Nat. Chem.* **2020**, *12*, 213-219.
- [14] Y. Rechkemmer, F. D. Breitgoff, M. van der Meer, M. Atanasov, M. Haki, M. Orlita, P. Neugebauer, F. Neese, B. Sarkar, J. van Slageren, *Nat. Commun.* **2016**, *7*, 10467.
- [15] E. A. Sutura, D. Maganas, E. Bill, M. Atanasov, F. Neese, *Inorg. Chem.* **2015**, *54*, 9948-9961.
- [16] a) F. Neese, *Wires. Comput. Mol. Sci.* **2012**, *2*, 73-78; b) F. Neese, *Wires. Comput. Mol. Sci.* **2018**, *8*, e1327.
- [17] This is realized by taking the direct product $B1 \times B2 = A2$, which shares the same symmetry as Lz in the $D2d$ point group, whereas Lx and Ly has the symmetry E ($u = x, y, z$) has the same transformation properties as the rotation operator R_u).
- [18] O. Kahn, *Molecular Magnetism*, Wiley, **1993**.
- [19] a) M. Atanasov, D. Ganyushin, K. Sivalingham, F. Neese, *Molecular Electronic Structures of Transition Metal Complexes II*, Springer, Verlag Berlin Heidelberg, **2012**; b) M. Atanasov, J. M. Zadrozny, J. R. Long, F. Neese, *Chem. Sci.* **2013**, *4*, 139-156.
- [20] In transition metals with an unquenched orbital angular momentum the energy separation between the Kramers' doublets are $L\lambda$, where λ is the atomic SOC constant
- [21] A. Genoni, *Acta Cryst. A.* **2020**, *76*, 172-179.
- [22] L. Krause, K. Tolborg, T. B. E. Grønbech, K. Sugimoto, B. B. Iversen, J. Overgaard, *J. Appl. Crystallogr.* **2020**, *53*, 635-649.
- [23] a) D. Maganas, S. Sottini, P. Kyritsis, E. J. J. Groenen, F. Neese, *Inorg. Chem.* **2011**, *50*, 8741-8754; b) J. M. Zadrozny, J. Teiser, J. R. Long, *Polyhedron* **2013**, *64*, 209-217; c) A. M. Thiel, E. Damgaard-Møller, J. Overgaard, *Inorg. Chem.* **2020**, *59*, 1682-1691.
- [24] a) G. A. Craig, M. Murrie, *Chem. Soc. Rev.* **2015**, *44*, 2135-2147; b) J. Ribas Gispert, *Coordination Chemistry*, Wiley-VCH, Weinheim, **2008**.
- [25] a) E. Espinosa, E. Molins, C. Lecomte, *Chem. Phys. Lett.* **1998**, *285*, 170-173; b) C. Gatti, *Z. Kristallogr.* **2005**, *220*, 399-457.

RESEARCH ARTICLE

Entry for the Table of Contents



Here, we have used the experimental electron density obtained from 20 K synchrotron X-ray diffraction data to quantify the zero-field splitting parameter in a Co(II) based single molecule magnet. The methodology uses the d-orbital populations to derive the ground state wavefunction composition, which is shown to be strongly correlated to the zero field splitting.